A New Methodology on Noise Equivalent Differential Temperature ($NE\Delta T$) Calculation for On-Orbit Advanced Microwave Sounding Unit–A Instrument

Banghua Yan and Stanislav Kireev

***Abstract*— A few deficiencies remain in the current NOAA Integrated Calibration/Validation System (ICVS) noise calculation method for characterizing Noise Equivalent Differential Temperature ($NE\Delta T$) performance of on-orbit Advanced Microwave Sounding Unit–A (AMSU-A) instruments. This ICVS method only accounts for the noise contribution resulting from one calibration parameter (warm count). The calculation is also dependent upon an assumption that the calibration gain equals to the sensitivity of warm count to temperature. In addition, the dependency of scene temperature is not considered. This study establishes a new methodology by accounting for the noise components resulting from all calibration parameters such as warm counts, warm target temperatures, space view (cold) counts and their covariance. Each noise component is computed using the product of the overlapping Allan deviation of corresponding parameter and the sensitivity of Earth scene temperature to the parameter. The new method also comprises the variation of scene temperature via scene count in noise estimation. For the AMSU-A instruments aboard the NOAA-18 to NOAA-19 and Metop-A to Metop-C satellites, the magnitudes of the orbital average $NE\Delta T$ calculated using the ICVS method exceed those from the new method by approximately 8% to 38%, corresponding to a range from 0.02 to 0.07K. Particularly, the deviations at the upper temperature sounding channels from 10 to 14 are around 0.05K. The magnitude of AMSU-A instrument noise can vary by around 18% for sounding channels and 40% for window channels due to scene temperature change. Therefore, the new method demonstrates its significant improvements in characterizing on-orbit AMSU-A instrument noise more accurately and comprehensively.**

***Index Terms*—Advanced Microwave Sounding Unit–A (AMSU-A) instrument noise ($NE\Delta T$), Microwave Humidity Sounder, data assimilation, error propagation, overlapping Allan deviation, and temperature dependency of instrument noise**

Manuscript received September 11, 2019, finally revised on October 24, 2020, and accepted on Jan. 2, 2021. This work was supported by the NOAA Center for Satellite Applications and Research (STAR). The manuscript contents are solely the opinions of the author(s) and do not constitute a statement of policy, decision, or position on behalf of NOAA or the U. S. Government.

I. INTRODUCTION

THE Advanced Microwave Sounding Unit-A (AMSU-A) instrument is a microwave radiometer consisting of 15 channels and its major specifications are shown in Table I [1]. The AMSU-A instrument has flown aboard NOAA-15 through NOAA-19 and Metop-A through Metop-C. AMSU-A offers key information on atmospheric and surface properties via three antenna units, A1-1, A1-2 and A2. A1-1 contains channels 6-7 and 9-15; A1-2 contains channels 3-5 and 8; and A2 contains channels 1 and 2. The 12 oxygen-band channels (channels 3-14) provide temperature soundings from the Earth's near-surface to an altitude of about 42 km. The remaining three "window" channels (channels 1, 2, and 15) aid the temperature sounding by correcting for the surface emissivity, atmospheric liquid cloud water, and total precipitable water. AMSU-A Sensor Data Record (SDR) data in past decades has contributed significantly to improving weather forecasts by Numerical Weather Prediction (NWP) Systems [2]-[6], retrieving environmental products [7], and monitoring climate change reliably [8].

An important parameter to characterize AMSU-A radiometer performance for these applications is the instrument noise, Noise Equivalent Differential Temperature ($NE\Delta T$), which represents the smallest temperature difference that an instrument can distinguish when looking at Earth scenes. This parameter helps weight satellite data by channel in the data error covariance matrix used by satellite Environmental Data Record (EDR) product retrieval systems [7] as well as NWP data assimilation systems [2]-[3]. In climate studies, instrument noise affects the detection of long-term climate trends of Earth-scene temperature data [9]-[10]. In practice, the AMSU-A measures the radiation from two calibration targets during every scan cycle [1]. The first one is the cosmic background

B. H. Yan is with the Satellite Calibration and Data Assimilation Branch in the Center for Satellite Applications and Research, National Oceanic and Atmospheric Administration, 5830 University Research Ct, College Park, MD 20740, USA (e-mail: Banghua.Yan@noaa.gov).

S. Kireev is with the Global Science Technologies Inc., College Park, MD 20742 USA (e-mail: Stanislav.Kireev@noaa.gov)

radiation (often called as "cold space"). The second one is an internal blackbody calibration target (often called as "warm load"). Measured radiometric counts corresponding to the warm load and the cold space are warm and cold counts respectively. The instrument noise can be affected by fluctuations in any of calibration target temperatures and counts, i.e., warm counts, cold counts, warm load Platinum Resistance Thermometers (PRT) temperature, and cold space temperature. However, the specifications in Table I do not provide any information regarding the temporal evolution of instrument noise resulting from fluctuations in calibration target parameters. Therefore, monitoring the noise performance of in-flight AMSU-A instruments is of paramount importance to a broader user community.

Table I AMSU-A Instrument Specifications [1].

Ch.	Center Frequency (MHz)	Bandwidth (MHz)	Temperature Sensitivity NEΔT (K)	Polarization
1	23800	270	0.3	V
2	31400	180	0.3	V
3	50300	180	0.4	V
4	52800	400	0.25	V
5	53596 ±115	170	0.25	H
6	54400	400	0.25	H
7	54940	400	0.25	V
8	55500	330	0.25	H
9	fo= 57290.344	330	0.25	H
10	fo ± 217	78	0.4	H
11	fo ± 322.2 ± 48	36	0.4	H
12	fo ± 322.2 ± 22	16	0.6	H
13	fo ± 322.2 ± 10	8	0.8	H
14	fo ± 322.2 ± 4.5	3	1.2	H
15	89000	1500	0.5	V

Currently, the noise performances of AMSU-A and other microwave instruments are routinely monitored in satellite instrument monitoring systems by national meteorological agencies such the American National Oceanic and Atmospheric Administration (NOAA), the European Organisation for the Exploitation of Meteorological Satellites (EUMETSAT) and the United Kingdom Met Office (UKMO). The instrument noise is characterized by the $NE\Delta T$ corresponding to the instrument warm load, which is computed from the quotient of the fluctuation (standard deviation or overlapping Allan deviation) of warm radiometric counts (or warm counts) and the calibration gain during one orbit of observations. Specifically, the Integrated Calibration/Validation System (ICVS) monitoring system in NOAA uses the overlapping Allan deviation [11]-[13], hereinafter referred to as the ICVS method. Recently, Hans et al. [14] offered a method, hereinafter named as Hans method, to assess the Microwave Humidity Sounder (MHS) instrument noise. This method is similar to the ICVS method except for an additional noise component resulting from cold counts among the MHS calibration targets. However, those methods show deficiencies in accurately characterizing onboard AMSU-A instrument noise. Firstly, the $NE\Delta T$ is converted based on an assumption that the calibration gain equals to the sensitivity of warm count parameter to temperature. This assumption does not work for an onboard instrument (see Sections II and IV). This is because the gain only denotes the ratio of the difference of two calibration target counts (i.e., warm counts and cold counts) to the difference of two calibration target temperatures [15]-[18]. In addition, the existing methods also neglect the noise contributions resulting from some calibration parameters as described in the last paragraph. Lastly, the variation of earth scene temperature is not taken into account, which is not consistent with noise feature of a pre-launch instrument. These deficiencies call for development of a new methodology on accurately characterizing in-flight AMSU-A instrument noise.

This study develops a new noise methodology for on-orbit AMSU-A instrument noise estimation by using the standard instrument calibration equation [16]-[18] and the error propagation formulas [19]. The new method accounts for the noise contributions resulting from all calibration parameters such as the warm count, cold counts, warm load PRT temperature, and cold space temperature. The final formula of the new method is acquired with certain simplifications based on assessments of each noise component by using AMSU-A measurements on NOAA-18, NOAA-19, Metop-A and Metop-B satellites. In addition, the new noise calculation formula is a function of earth scene temperature. Moreover, this study employs the new method to analyze the temperature dependence of on-orbit AMSU-A instrument noise performance and the theoretical limitations of the existing methods. Following it, we apply all of the new formula and two existing methods to the above four legacy AMSU-A instruments to quantify the noise errors caused by the existing methods. The lifetime noise performance of Metop-C AMSU-A instrument is also assessed.

After this section, Section II briefs the nature of the problem in the gain-based noise calculation methods (i.e., ICVS and Hans methods). Section III introduces the new noise computation formula for an onboard AMSU-A instrument. Section IV discusses advantages of the new method over the ICVS and Hans methods. Section V analyzes the orbital averaged AMSU-A instrument noise performance by applying the ICVS, Hans and new methods to NOAA-18 to NOAA-19, and Metop-A to Metop-C. Section VI provides a summary and conclusions.

II. Nature of the Problem in the Existing Methods

The two gain-based computation methods, i.e., the ICVS in [11] and the Hans method in [14], have been widely adopted to monitor the noise performance of in-flight AMSU-A instruments and other microwave instruments.

According to the ICVS method [11], the orbital AMSU-A instrument noise, $NE\Delta T_{C_W}^{ICVS}$, is expressed to be

$$NE\Delta T_{C_W}^{ICVS} = \sqrt{\frac{1}{4(N-2)}\sum_{i=1}^{N-1}\frac{1}{\overline{G_0(i)}^2}\left[\left(C_{W_1}(\mathrm{i}+1)-C_{W_1}(\mathrm{i})\right)^2+\left(C_{W_2}(\mathrm{i}+1)-C_{W_2}(\mathrm{i})\right)^2\right]} \quad (1)$$

where N is the number of scans per orbit; 'i' is the scan index per orbit; C_{W_1} and C_{W_2} denote the first and second samples of the radiometric warm counts per scan. The index of the channel is omitted throughout this study for clarity.

In addition, the $\overline{G_0(i)}$ represents the channel gain, an averaged sensitivity about two calibration target count parameters to temperature per scan, which is expressed by

$$\overline{G_0(i)} = \left| \frac{\left(\overline{C_W(i)} - \overline{C_C(i)}\right)}{\left(\overline{T_W(i)} - \overline{T_C(i)}\right)} \right|, \qquad (2)$$

where $\overline{C_C(i)}$ *and* $\overline{C_W(i)}$ are the average of 2 samples of cold and warm counts per scan respectively; $\overline{T_W(i)}$ is the average of 5 or 7 samples of warm load PRT temperatures per scan. The scan index 'i' in the variables are frequently omitted for clarity in the following analyses.

The Hans method was originally developed for calculating MHS scene noise based on a linear interpolation of cold and warm count noise components, each of which is computed using a scheme similar to the ICVS method. By extending it to AMSU-A, the noise is expressed as

$$NE\Delta T_A^{Hans} = NE\Delta T_{C_C}^{ICVS} + (T_A - Tc)\frac{\left(NE\Delta T_{C_W}^{ICVS} - NE\Delta T_{C_C}^{ICVS}\right)}{(T_W - Tc)}, \qquad (3)$$

where $NE\Delta T_{C_W}^{ICVS}$ is evaluated using (1); $NE\Delta T_{C_C}^{ICVS}$ adopts the same approach as that of $NE\Delta T_{C_W}^{ICVS}$ but for cold counts, i.e.,

$$NE\Delta T_{C_C}^{ICVS} = \sqrt{\frac{1}{4(N-2)}\sum_{i=1}^{N-1}\frac{1}{\overline{G_0(i)}^2}\left[\left(C_{C_1}(\mathrm{i}+1) - C_{C_1}(\mathrm{i})\right)^2 + \left(C_{C_2}(\mathrm{i}+1) - C_{C_2}(\mathrm{i})\right)^2\right]}, \qquad (4)$$

where C_{C_1} and C_{C_2} denote the first and second samples of the cold counts per scan. Other variables are referred to the above explanations.

These two methods have a key problem. They converted the fluctuation in the warm and cold counts into $NE\Delta T$ (the fluctuation in temperature) by using the channel gain. The accuracy of this conversion is subject to the assumption that the gain needs to equal to the sensitivity of the warm counts and the cold counts to temperature. However, in fact, this assumption does not work for an onboard AMSU-A instrument. The SDR data from AMSU-A instruments onboard NOAA-18 to NOAA-19, and Metop-A to Metop–B reveal that warm counts and cold counts typically vary by different magnitudes with each scan, though they display a similar cyclical pattern with every orbit. Fig.1 shows a time series of ΔC_W and ΔC_C for 150 scans for channel 2 of AMSU-A onboard NOAA-18/19 and Metop-A/B. Here, $\Delta C_W(i) = C_W(i) - C_W(i-1)$, $\Delta C_C(i) = C_C(i) - C_C(i-1)$, and $i = 2 \sim N$. The limited 150 scans are used to provide observable differences of ΔC_W and ΔC_C in magnitude. From the time series of ΔC_W and ΔC_C, their differences distribute primarily within a few counts depending upon scan position and channel. This inconsistent count change with scan can result in different sensitivities of warm and cold counts individually to temperature. Moreover, each of those sensitivities deviates from the calibration gain, causing errors in computing $NE\Delta T$ (see Section IV.B).

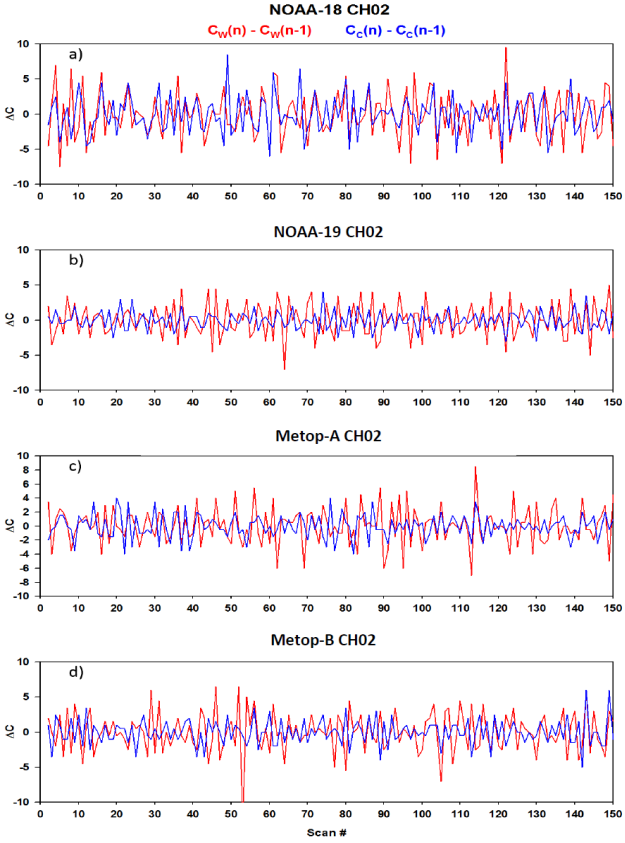

Fig. 1. Time series of the variation of warm counts (C_W) and cold counts (C_C) within 150 scan lines (X-axis) of the data sets between two neighboring scan lines (single Allan deviation) for AMSU-A channel 2 on-board NOAA-18 through Metop-B satellites. Symbols in (a) and scan number (#) in X-axis' title in (d) are applied to all sub-graphs in the figure.

III. New $NE\Delta T$ Formula for In-flight AMSU-A Instruments

Below, we first derive the expression consisting of noise contributions occurred in all calibration target parameters for on-orbit AMSU-A instrument. Then, we assess the magnitude of each noise component to produce a simplified noise calculation formula.

A. Development of New $NE\Delta T$ Formula

In theory, the noise of a radiometer is related to a series of instrumental quantities (e.g., radiometer system noise temperature, pre-detection bandwidth, and integration time [20]). In practice, some of these parameters, such as the system noise temperature, are not easily accessible for both pre-launch and post-launch instruments. The instrument noise for a pre-

launch radiometer is calculated from the standard deviation of the radiometer output (in Kelvins) when an antenna system is viewing a reference scene target at 300K [21]. However, this approach is not applicable for onboard instrument noise calculations. It is difficult, if not impossible, to determine the standard deviation of the radiometer output, such as antenna temperature T_A, because variable Earth atmospheric and surface properties determine changes in measured T_A for onboard AMSU-A instruments. Instead, in-flight AMSU-A instrument noise is currently calculated by statistical estimations (either overlapping Allan deviation or standard deviation) of warm counts, which are further converted into the $NE\Delta T$ using the calibration gain [11]. Our study still utilizes the approach of overlapping Allan deviation to quantify statistical fluctuations of a parameter. The improvement is to take each of the major noise sources in the calibration target parameters into account of instrument noise estimation. More importantly, Allan deviation of each parameter is converted into a corresponding noise component by using the sensitivity of the parameter to temperature, as analyzed below.

In AMSU-A observations, the radiometer output, the antenna temperature of an Earth-scene, T_A, is determined using a nonlinear calibration equation, i.e., [16]-[17]

$$T_A = T_W + (T_W - T_C)\frac{(C_S - C_W)}{(C_W - C_C)} + \mu(T_W - T_C)^2\frac{(C_S - C_W)(C_S - C_C)}{(C_W - C_C)^2}, \quad (5)$$

where C_C, C_W *and* C_s denote the cold space, warm target and Earth-scene radiometric counts respectively; T_C and T_W denote the cold space and warm target PRT temperatures respectively; and μ denotes the nonlinear coefficients. The indices of channel and scan line are regularly omitted in (5) and subsequent equations throughout the manuscript for clarity unless otherwise described. Strictly speaking, the above calibration equation should be generalized using radiance, instead of temperature, which is important especially for high frequencies. However, this is not necessary for the computation of the noise. According to our calculations, resultant noise errors using temperature instead of radiance are trivial for instrument noise accuracy at 15 AMSU-A channels (an error of approximately 0.1% to 0.5% depending upon channel). This is because only the difference of the warm and cold calibration target temperatures are involved in the calculation of the noise in the new method (see Appendix A). The output of AMSU-A antenna temperature data record (TDR) in operational processing stream is in temperature instead of radiance. Therefore, the calibration equation and follow-up noise calculation formulae are derived in terms of temperatures instead of radiance to avoid the transition between radiance and temperature.

According to the formulas of error propagation [19] and Eq. (5), we can derive the following equation

$$NE\Delta T_A^{New} = \sigma_{T_A}^{A,} = \sqrt{(NE\Delta T_{C_W})^2 + (NE\Delta T_{C_C})^2 + (NE\Delta T_{T_W})^2 + \delta_{Cov(C_W,C_C)} + \delta_{Cov(C_W,T_W)} + \delta_{Cov(C_C,T_W)},} \quad (6)$$

where the first three components represent three independent noise components corresponding to the warm counts, the cold counts, and the warm load temperatures respectively, hereinafter termed the warm count noise, cold count noise, and warm temperature noise for clarity unless otherwise mentioned. As given in Appendix A, each of them is proportional to the product of the sensitivity of T_A to the calibration parameter (e.g., $\frac{\partial T_A}{\partial C_W}$) and the overlapping Allan deviation of the calibration parameter (e.g., $\sigma_{C_W}^A$), seeing (A4-1) ~ (A4-3). The other three noise components consist of covariance items that can be positive or negative depending on proportional or inverse relationships among the relevant parameters. The derivation of the equation is given in appendix A. The cold space temperature, T_C, denotes the cosmic temperature after removing the correction of antenna side lobe interference on cold space temperature via the Earth limb and spacecraft as well the nonlinearity of instrument square-law detector [21]. The magnitudes of T_C at the AMSU-A channels are only a few Kelvins [21][22]. Because of its trivial contribution into NEΔT, the noise component due to cold space temperature variations is not counted in the above derivation (see Section III. B for more discussions).

To examine the possibility of a simple expression, it is important to understand if all noise components, including the nonlinear items within each component, are essential or not for in-flight AMSU-A instrument noise performance, as given in the following sub-section.

B. Assessment of Noise Components

To understand the contribution of each noise component, we select three days of the data for each of the AMSU-A instruments onboard NOAA-18, NOAA-19, Metop-A, and Metop-B. A different period of the data sets per satellite instrument are used to exemplify ordinary cases as well as extremely anomalous cases with noteworthy parameter instabilities. The extremely noise data are included to ensure that the simplified formula is still valid even as the noise is very strong. The dates of the data sets for NOAA-18, NOAA-19, Metop-A, Metop-B are 03/05 ~ 03/08/2018, 10/04 ~ 10/07/2017, 05/27 ~ 05/30/2017, 10/16 ~ 10/19/2016 correspondingly. In addition to the six noise components in (6), we also include a nonlinear noise item, $(NE\Delta T_A)_{NL}$, which is a combined contribution due to all nonlinear portions associated with the above noise components, as given in (B12).

In the following analysis, seven noise components are computed based on the average for an entire orbit of the data (orbital averaging) to ensure the consistency of the results to the NOAA operational monitoring system. For clarity, 'orbital averaging" is mostly omitted in the rest of the manuscript unless otherwise mentioned. The computation procedures of the seven noise components i.e., $NE\Delta T_{C_W}$, $NE\Delta T_{C_C}$, $NE\Delta T_{T_W}$, $\delta_{Cov(C_W,C_C)}$, $\delta_{Cov(C_W,T_W)}$, $\delta_{Cov(C_C,T_W)}$, and $(NE\Delta T_A)_{NL}$, are provided in Appendix B. Table II illuminates the three-day mean of all orbital averages for $NE\Delta T_A^{New}$ and seven noise components at 15 channels for the four legacy

satellite instruments. The $(NE\Delta T_A^{New})_L$ in the table will be discussed later [see (8) below]. Several important conclusions are summarized based on the results in the table.

Table II Three day-mean of $NE\Delta T_A^{New}$, $NE\Delta T_{C_W}$, $NE\Delta T_{C_C}$, $NE\Delta T_{T_W}$, $\delta_{Cov(C_W,C_C)}$, $\delta_{Cov(C_W,T_W)}$, $\delta_{Cov(C_C,T_W)}$, $(NE\Delta T_A)_{NL}$ and $(NE\Delta T_A^{New})_L$ at 15 channels for Metop-B AMSU-A. The magnitude of each item is rounded to the thousandth decimal place; the covariance items have the unit of Kelvin^2, while the unit of other items are in Kelvin.

Ch.#	$NE\Delta T_A^{New}$	$NE\Delta T_{C_W}$	$NE\Delta T_{C_C}$	$NE\Delta T_{T_W}$	$\delta_{Cov(C_W,C_C)}$	$\delta_{Cov(C_W,T_W)}$	$\delta_{Cov(C_C,T_W)}$	$(NE\Delta T_A)_{NL}$	$(NE\Delta T_A^{New})_L$
1	0.136	0.129	0.040	0.003	0.017	0.000	0.000	-0.001	0.136
2	0.147	0.139	0.045	0.003	0.015	0.000	0.000	-0.001	0.147
3	0.222	0.219	0.027	0.003	0.023	0.000	0.000	-0.001	0.222
4	0.140	0.138	0.013	0.003	0.015	0.000	0.000	-0.001	0.140
5	0.127	0.126	0.012	0.003	0.010	0.000	0.000	0.000	0.127
6	0.110	0.108	0.015	0.003	0.012	0.000	0.000	-0.002	0.110
7	0.110	0.108	0.020	0.003	0.013	0.000	0.000	-0.002	0.110
8	0.131	0.128	0.027	0.003	0.014	0.000	0.000	-0.001	0.131
9	0.118	0.115	0.025	0.003	0.006	0.000	0.000	-0.002	0.118
10	0.156	0.153	0.030	0.003	0.001	0.001	0.000	-0.002	0.156
11	0.177	0.175	0.030	0.003	0.008	0.001	0.000	-0.003	0.177
12	0.264	0.261	0.037	0.003	0.003	0.000	0.000	-0.005	0.264
13	0.377	0.375	0.042	0.003	0.004	0.000	0.000	-0.007	0.377
14	0.639	0.637	0.053	0.003	-0.002	0.001	0.000	-0.011	0.640
15	0.119	0.116	0.021	0.003	0.012	0.000	0.000	-0.001	0.119

Firstly, among the three independent noise components, the $(NE\Delta T_{C_W})^2$ contributes the most to the $(NE\Delta T_A^{New})^2$. Typically, it is above 80% for all channels for the four satellite AMSU-A instruments thus dominating the magnitude of the noise. In contrast, the magnitude of $(NE\Delta T_{C_C})^2$ is usually less than 10%. This is caused partially by a relatively low temperature sensitivity to cold count, where the distribution of $\left|\frac{\partial T_A}{\partial C_W}\right|$ lies approximately from 0.04 to 0.2K per count and $|\frac{\partial T_A}{\partial C_C}|$ is usually smaller than 0.01K per count based on our analyses (the graph is omitted). Additionally, the contribution of $(NE\Delta T_W)^2$ is usually less than 0.5%. The change in warm load PRT temperature with scan is approximately two orders of magnitude smaller than the changes of radiometric counts of two calibration targets (refer to the NOAA ICVS web site). As a result, the $|\sigma_{T_W}^A|$ in this noise component [see A4-3)] is much smaller than the $|\sigma_{T_C}^A|$, thus producing a small amount of $(NE\Delta T_W)^2$.

Secondly, $\delta_{Cov(C_W,C_C)}$ is the largest contributor among the three covariance noise components. This is because the absolute magnitude of $\delta_{Cov(C_W,C_C)}$ is up to 0.02K^2, which is about 10% of $(NE\Delta T_A^{New})^2$ although the contribution of the remaining two covariance terms is around ±0.1%. This conclusion is consistent with the design of the instrument calibration targets. For the AMSU-A instrument, either warm or cold counts of two in-flight targets are measured from an analog-to-digital converter (ADC). Fluctuations of the counts are sensitive primarily to changes in the instrument temperature [21]. Consequently, warm and cold counts per channel display a similar orbital cycle pattern due to the diurnal cycle of instrument temperature (refer to the ICVS website). In contrast, the in-flight warm load PRT temperature is measured from a PRT sensor that is digitized via a different A/D converter aboard the AMSU-A, where the count is converted into a temperature via the count-to-resistance and resistance-to-PRT temperature parameters [16][17]. The covariance of warm and cold count anomalies with the warm PRT temperature anomaly is thus relatively weak.

Thirdly, the contribution of $(NE\Delta T_A)_{NL}$ is about -0.001K that is around -0.3% (see Table II), and is negligible compared with the contributions of other noise components. This is primarily because the whole nonlinearity item in the calibration equation (5) is at most a couple of Kelvins [16][21]. Meanwhile, this feature can explain why the contribution of the noise component due to the instability of cold space temperature (T_C), i.e., $NE\Delta T_{T_C}$, is negligible, as given below.

By using the linearity portion in (5), we have

$$NE\Delta T_{T_C} = \left|\frac{\partial T_A}{\partial T_c}\sigma_{T_c}^A\right|. \quad (7)$$

In (7), $\left|\frac{\partial T_A}{\partial T_c}\right| \approx \left|\frac{(C_S-C_W)}{(C_W-C_C)}\right| \ll \left|\frac{\partial T_A}{\partial T_c}\right| \approx 1+\frac{(C_S-C_W)}{(C_W-C_C)} \sim 1.0$ because $\left|\frac{(C_S-C_W)}{(C_W-C_C)}\right| \ll 1.0$. Meanwhile, the magnitude of $\sigma_{T_c}^A$ is small. T_C represents the cold space brightness temperature that equals to the cosmic temperature after removing the correction of antenna side lobe interference via the Earth limb and spacecraft as well the nonlinearity of instrument square-law detector. The analyses in [21][22] show that the contribution from the antenna side lobe interference with the Earth limb and spacecraft should be computed using actual earth scene temperature, thus being a changeable correction along with location. However, in the current operational processing system for all AMSU-A TDR observations, a fixed correction is used to reduce the contamination from the antenna sidelobe interference with the Earth limb and spacecraft. The error due to this fixed correction is on the order of 0.5K, which is similar to that in warm load

PRT temperatures. The noise component of cold space temperature, i.e., $NE\Delta T_{T_C}$, is even smaller than the warm load temperature noise component ($NE\Delta T_W$), being a negligible contribution.

Therefore, based on the above analyses, (6) can be further simplified as follows:

$$(NE\Delta T_A^{New})_L = \sqrt{\left[(\frac{\partial T_A}{\partial C_W})_L(\sigma_{C_W}^A)_L\right]^2 + \left[(\frac{\partial T_A}{\partial C_C})_L(\sigma_{C_C}^A)_L\right]^2 + 2(\frac{\partial T_A}{\partial C_W})_L(\frac{\partial T_A}{\partial C_C})_L cov(C_W, C_C)}, \quad (8)$$

$$(\frac{\partial T_A}{\partial C_W})_L = \frac{(T_W - T_C)(C_C - C_S)}{(C_W - C_C)^2}, \quad (9\text{-}1)$$

$$(\frac{\partial T_A}{\partial C_C})_L = \frac{(T_W - T_C)(C_S - C_W)}{(C_W - C_C)^2}, \quad (9\text{-}2)$$

where the subscript 'L' means that all noise components in (8) are determined by a linear calibration equation. In other words, the items related to the nonlinear coefficient μ in (A4-7) through (A4-9) are neglected in each partial derivative, as shown in (9-1) and (9-2). To confirm the accuracy of (8), Table II also includes the three-day mean of the orbital $(NE\Delta T_A^{New})_L$. The results show that the three-day average of $(NE\Delta T_A^{New})_L$ are almost identical to those found by using (6). Because the contributions of the neglected nonlinear and two covariant noise components are small and typically have different signs, they mostly cancel each other out.

A simplified but still accurate formulation has been derived to evaluate onboard AMSU-A instrument noise performance, which consists of three major noise components, i.e., the warm and cold count noise components and their covariance. Each noise component is calculated separately based on the sensitivity of each related calibration parameter to temperature.

IV. Discussions about Advantages of New Method

The new method is used below to identify the temperature dependency of on-orbit AMSU-A instrument noise performance. Following it, it is also utilized to address deficiencies of the ICVS and Hans Methods.

A. Dependency of Instrument Noise upon Scene Temperature

In light of the new formula in (8), for a given channel, the on-orbit instrument noise can exhibit the dependency on scene temperature T_A through changeable sensitivity of the calibration parameters to scene temperature, e.g., $|(\frac{\partial T_A}{\partial C_W})_L|$ and $|(\frac{\partial T_A}{\partial C_C})_L|$. According to the above analysis (see Appendix A), $|(\frac{\partial T_A}{\partial C_W})_L|$ is proportional to $|(C_C - C_S)|$, while $|(\frac{\partial T_A}{\partial C_C})_L|$ is proportional to $|(C_S - C_W)|$. According to our analyses, the magnitude of $|(C_C - C_S)|$ can typically vary by 10% for sounding channels among global observations of AMSU-A and the magnitude can be up to 30% for window channels. This variation may cause the dependency of instrument noise on scene temperature.

In practice, however, it is challenging to evaluate the dependency of instrument noise ($NE\Delta T_A$) on T_A based on an orbital average of AMSU-A observations as the ICVS method does, because T_A changes largely within one orbit. As a result, instead of using an orbital average, we introduced a bin-averaged instrument noise, where each bin of the data set can be constructed according to a certain scene temperature range. To reduce impact of highly noisy data on the analysis, we only use the Metop-B AMSU-A data in the Section III.B for the analysis of the noise temperature dependency.

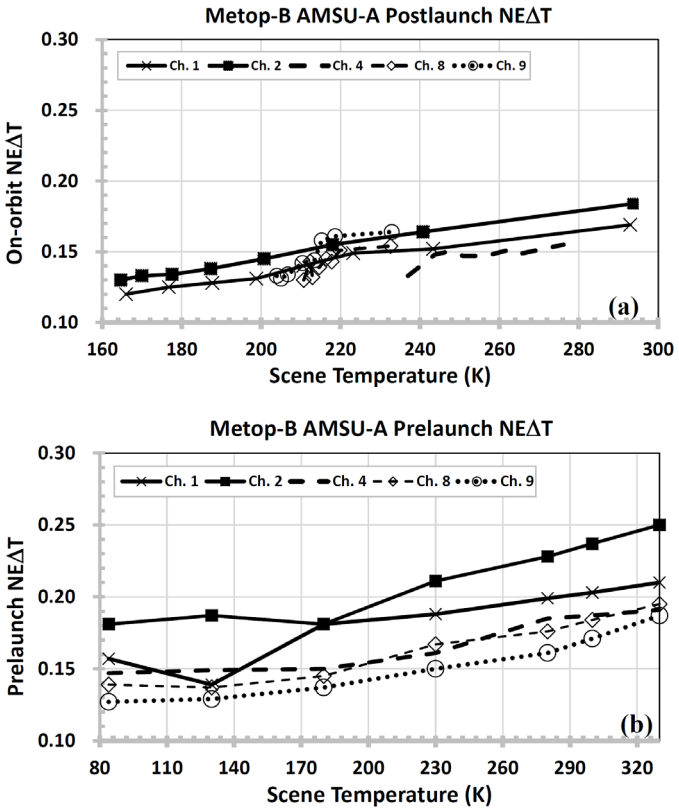

Fig. 2. Metop-B AMSU-A Instrument noise at channels of 1, 2, 4, 8, and 9 as a function of scene temperature. (a). Three-day averages of post-launch bin-based instrument noise as a function of an averaged scene temperature, where the three-day mean is computed using all bin-based $NE\Delta T_A$ values with a similar temperature range during three days that span from 16 -19 October, 2016. (b) Prelaunch instrument noise at 18°C of instrument temperature as a function of scene temperature [21].

With the data sets for Metop-B AMSU-A, each day of observations per channel are re-grouped into 8 bins according to different ranges of T_A from lowest to highest scene temperatures. Eight bins are categorized to ensure that each bin contains sufficient and about the same number of samples for a statistical analysis. The data per bin can come from multiple orbits per day, but any sub-data sets per orbit for a given temperature range are not used if the number of covered scans is less than 100. As a result, the total number of scans used in the bin-averaged $NE\Delta T_A$ is approximately half of the original data sets. By applying (8) to each bin of the data, we computed all bin-based $NE\Delta T_A$ for all channels. Results show that the bin-averaged instrument noise for sounding channels varies approximately around 18% regarding 50K or less of temperature change. The bin-averaged instrument noise for

window channels varies approximately 40% due to approximate 130K of temperature change. The variation range of the noise temperature dependency is actually higher than that of either $|(\frac{\partial T_A}{\partial C_W})_L|$ or $|(\frac{\partial T_A}{\partial C_C})_L|$. This increased range is primarily because of the instability of warm and cold counts due to an abundance of noisy data, i.e., large $(\sigma^A_{C_W})_L$ and $(\sigma^A_{C_C})_L$ at some bins. As an example, Fig. 2a shows three-day averaged bin instrument noise per certain scene temperature range at channels 1, 2, 4, 8, and 9 (at least one channel per AMSU-A1-1, A1-2 and A2) as a function of averaged scene temperature for Metop-B AMSU-A. The magnitudes of $NE\Delta T_A$ at channels 1, 2, 4, 8 and 9 change approximately 41.8%, 41.5%, 16.5%, 18.5%, 23.3% respectively.

The scene temperature dependency of AMSU-A instrument noise is also observed in prelaunch. Fig. 2b displays the Metop-B AMSU-A prelaunch instrument noise at 18°C for the same channels as those in Fig. 2a. The range of scene temperature change in prelaunch is larger than that in post-launch in particular for sounding channels. For the similar temperature range to that in Fig. 1a, the prelaunch instrument noises at channel 1, 2, 4, 8 and 9 increase by 12.2%, 30.9%, 14.9%, 5.4% and 7.3% respectively. Generally, prelaunch instrument noise shows a smaller change with scene temperature than post-launch instrument noise. This difference is caused primarily by noisy warm and cold counts for the selected data sets due to instrument anomalies.

The new method has demonstrated the temperature dependency of onboard instrument noise well consistent with the noise feature of prelaunch instrument. At present, the instrument noise for AMSU-A and other microwave instruments aboard satellite platforms is estimated using an orbit-based average [11]. Orbit-averaged scene temperatures at AMSU-A channels distribute usually from 210K to 260K, which are colder than the reference temperature of 300K for standard prelaunch instrument noise [21]. Therefore, future onboard instrument noise assessment should consider the noise change resulting from the temperature deviation of the orbital average from the reference temperature 300K to better compare with the standard prelaunch instrument noise.

B. Limitations of ICVS and Hans Methods

The limitations of the current noise calculation methods are related to scenarios where an instrument is used. The use of an instrument can be categorized into three types of scenarios. As presented in Figs. 3a through 3c, the line $\overline{CW}$ represents scenario 1, which corresponds to an ideal instrument, where C_C and C_W are invariant with scan (i.e., $\Delta C_W = \Delta C_C = 0.0$). The line $\overline{C'W'}$ denotes scenario 2, which corresponds to a pre-launch instrument, where C_C and C_W can change, but the two variations are identical (i.e., $\Delta C_W = \Delta C_C \neq 0.0$). The line $\overline{C''W''}$ is for scenario 3, which corresponds to a post-launch instrument, where C_C and C_W vary differently (i.e., $\Delta C_W \neq \Delta C_C \neq 0.0$). ΔC_W and ΔC_C are defined as follows: $\Delta C_W(i) = C_W(i) - C_W(i-1)$, $\Delta C_C(i) = C_C(i) - C_C(i-1)$, and $i = 2 \sim N$, where the index 'i' denotes the ith scan and N denotes the number of the scans per orbit.

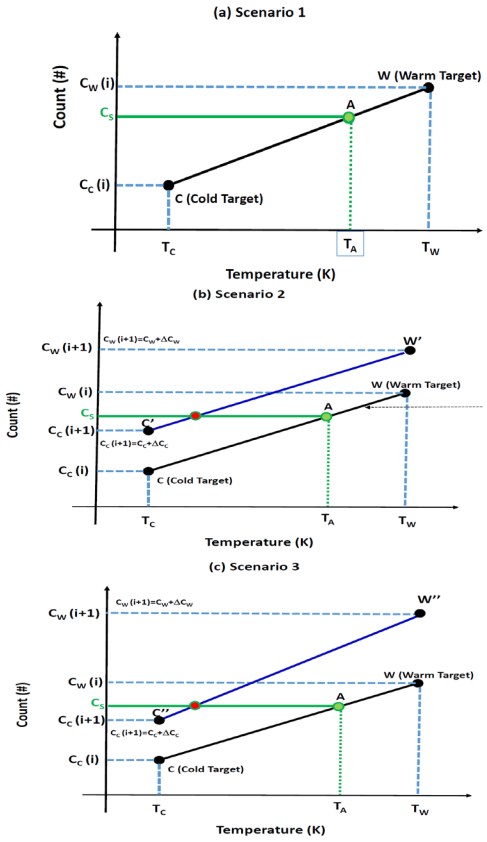

Fig. 3. AMSU-A linear calibration sketch under three scenarios for a given Earth-scene count C_S. (a) Scenario 1: the line $\overline{CW}$ represents for the position with invariant C_C and C_W during calibration process. (b) Scenario 2: $\overline{C'W'}$ the position with the same change in both C_C and C_W with scan line, i.e., $\Delta C_W = \Delta C_C \neq 0.0$. (c) Scenario 3: $\overline{C'W''}$ the position with dissimilar changes in both C_C and C_W, i.e., $\Delta C_W \neq 0.0$, $\Delta C_C \neq 0.0$ and $\Delta C_W \neq \Delta C_C$.

Scenario 1: $\Delta C_W = \Delta C_C = 0.0$

This depicts an idealized instrument noise performance where warm and cold counts are constant. According to (A5) in Appendix A and (B10) in Appendix B, we have that $(\sigma^A_{C_W})_L = (\sigma^A_{C_C})_L = cov(C_W, C_C) = 0.0$ as $\Delta C_W = \Delta C_C = 0.0$. Further, we have that $(NE\Delta T_A^{New})_{L,\ Scenario\ 1} = 0.0$, i.e., no noise in measurements. Alternatively, according to the ICVS method [11], the instrument noise is zero because the Allan deviation of warm counts is zero. Besides, the solid line $\overline{CW}$ has a constant slope of $G_{\overline{CW}}$ and its slope equals the calibration gain, i.e., $G_{\overline{CW}} = \frac{(C_W - C_C)}{(T_W - T_C)} = G_0$. Therefore, the new method is replaceable with the ICVS method under scenario 1 that corresponds to a noise-free instrument.

Scenario 2: $\Delta C_W = \Delta C_C \neq 0.0$

This represents an instrument noise performance where the variations of warm count and cold count along with scan within 'satellite' observations are always identical, which typically corresponds to a pre-launch instrument performance.

For the new method, as $\Delta C_W = \Delta C_C \neq 0.0$, we obtain the following relations according to (A5) and (B10).

$$(\sigma^A_{C_W})_L = (\sigma^A_{C_C})_L, \qquad (10\text{-}1)$$

$$cov(C_W, C_C) = (\sigma^A_{C_W})_L \cdot (\sigma^A_{C_C})_L = \left[(\sigma^A_{C_W})_L\right]^2. \quad (10\text{-}2)$$

Furthermore, we obtain

$$G_{SC2} = \left|\frac{d(T_A)_L}{\Delta C_W}\right|^{-1} = G_0 = \frac{(C_W - C_C)}{(T_W - T_C)} \quad (11\text{-}1)$$

Alternatively, according to the geometry in the figure, we also derive

$$G_{\overline{C'W'}} = \frac{(C_W + \Delta C_W) - (C_C + \Delta C_C)}{(T_W - T_C)} = \frac{C_W - C_C}{(T_W - T_C)} = G_0. \quad (11\text{-}2)$$

Both (11-1) and (11-2) demonstrate that the new slope, $G_{\overline{C'W'}}$, is the same as that in scenario 2. In other words, the instantaneous sensitivity of the two target counts to the temperature under scenario 2 equals to the calibration gain G_0.

Furthermore, by inserting (10-1) and (10-2) into (8), we obtain

$$(NE\Delta T_A^{New})_{L,\ Scenario\ 2} = \sqrt{(\sigma^A_{C_W})^2_L[(\frac{\partial T_A}{\partial C_W})_L + (\frac{\partial T_A}{\partial C_C})_L]^2} = NE\Delta T^{ICVS}_{C_W}, \quad (12)$$

which implies that the new method is also exchangeable with the ICVS method under scenario 2.

Scenario 3: $\Delta C_W \neq \Delta C_C, \Delta C_W \neq 0.0, \Delta C_C \neq 0.0$

The scenario 3 corresponds to a post-launch instrument, where $\Delta C_W \neq \Delta C_C, \Delta C_W \neq 0.0, \Delta C_C \neq 0.0$, and typically $|\Delta C_W| > |\Delta C_C|$, as shown in Fig. 1 above. The conclusions from (10-1) through (12) in Scenario 2 are not applicable for the Scenario 3.

For Scenario 3, the slope of the line $\overline{C''W''}$, $G_{\overline{C''W''}}$, does not equal the calibration gain:

$$G_{\overline{C''W''}} = \frac{(C_W + \Delta C_W) - (C_C + \Delta C_C)}{(T_W - T_C)} = \frac{(C_W - C_C)}{(T_W - T_C)} + \frac{(\Delta C_W - \Delta C_C)}{(T_W - T_C)} > G_0. \quad (13\text{-}1)$$

where $G_{\overline{C''W''}}$ represents the overall count sensitivity to temperature.

Using (B6) and (B7), we have

$$\left|\overline{(\frac{\partial T_A}{\partial C_W})_L}\right| = \left|\frac{(\overline{C_C} - \overline{C_S})}{(\overline{C_W} - \overline{C_C})}\right| \frac{1}{G_0} < \frac{1}{G_0}, \quad (13\text{-}2)$$

$$\left|\overline{(\frac{\partial T_A}{\partial C_C})_L}\right| = \left|\frac{(\overline{C_W} - \overline{C_S})}{(\overline{C_W} - \overline{C_C})}\right| \frac{1}{G_0} < \frac{1}{G_0}, \quad (13\text{-}3)$$

where the scan index 'i' is omitted. Thus, the sensitivity of either warm or cold counts to temperature is smaller than the inverse of the gain. This means that the gain is larger than the sensitivity of temperature to warm (cold) counts. Hence, both the ICVS and Hans methods use the gain to represent the sensitivity of individual warm (cold) counts to temperature, thus causing a positive noise calculation error.

In addition, for Scenario 3, $(\sigma^A_{C_W})_L \neq (\sigma^A_{C_C})_L$. As a matter of fact, the orbital Allan deviation of warm counts is persistently greater than that of cold counts because $|\Delta C_W| > |\Delta C_C|$ for the vast scans per orbit. Fig. 4 displays the time series of orbital Allan deviations at channels 2, 8, and 9 for Metop-B AMSU-A instrument. Approximately 0.5K exists between two $(\sigma^A_{C_W})_L$ and $(\sigma^A_{C_C})_L$. This conclusion except for a slightly different amount is applicable to other channels and AMSU-A instruments onboard other satellites.

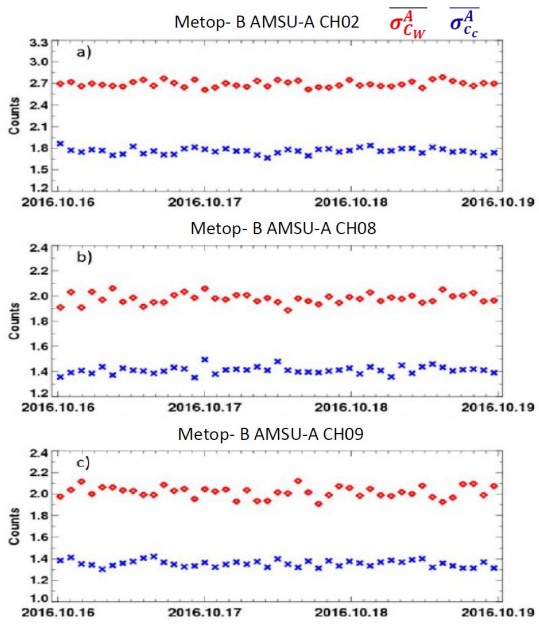

Fig. 4. Time series of the orbital average of Allan deviations for warm count ($\overline{\sigma^A_{C_W}}$) (see 'diamond') and cold count ($\overline{\sigma^A_{C_C}}$) (see 'cross') at the three channels for Metop-B AMSU-A during three days of the data sets. (a) Ch. 2. (b) Ch. 8. (c) Ch. 9.

For the convenience of the following discussion, we introduce a variable $\Delta_1 = (\sigma^A_{C_W})_L - (\sigma^A_{C_C})_L$, which denotes the difference between two overlapping Allan deviation based on the warm counts and the cold counts. Given (8) and $(\sigma^A_{C_C})_L = (\sigma^A_{C_W})_L - \Delta_1$, we have:

$$(NE\Delta T_A^{New})_{L,Scenario\ 3} = \sqrt{\left[(\frac{\partial T_A}{\partial C_W})_L(\sigma^A_{C_W})_L\right]^2 + \left\{(\frac{\partial T_A}{\partial C_C})_L[(\sigma^A_{C_W})_L - \Delta_1)]\right\}^2 + 2(\frac{\partial T_A}{\partial C_W})_L(\frac{\partial T_A}{\partial C_C})_L(\sigma^A_{C_W})_L[(\sigma^A_{C_W})_L - \Delta_1)]}. \quad (14)$$

Furthermore,

$$(NE\Delta T_A^{New})_{L,\ Scenario\ 3} = \sqrt{(\frac{1}{G_0})^2(\sigma^A_{C_W})^2_L + \delta} = \sqrt{NE\Delta T^{ICVS}_{C_W} + \delta} \quad (15\text{-}1)$$

with

$$\delta = \Delta_1 \cdot \left\{\Delta_1 \cdot \left[\left(\frac{\partial T_A}{\partial C_C}\right)_L\right]^2 - 2(\sigma^A_{C_W})_L\left(\frac{\partial T_A}{\partial C_C}\right)_L(\frac{\partial T_A}{\partial C_W})_L - 2(\sigma^A_{C_W})_L\left[\left(\frac{\partial T_A}{\partial C_C}\right)_L\right]^2\right\}. \quad (15\text{-}2)$$

According to our analysis (omitted), it is demonstrated that

$$\Delta_1 \cdot \left[\left(\frac{\partial T_A}{\partial C_C}\right)_L\right]^2 < 2(\sigma^A_{C_W})_L\left(\frac{\partial T_A}{\partial C_C}\right)_L\left(\frac{\partial T_A}{\partial C_W}\right)_L + 2(\sigma^A_{C_W})_L\left[\left(\frac{\partial T_A}{\partial C_C}\right)_L\right]^2 \quad (16\text{-}1)$$

or

$$\delta < 0.0. \quad (16\text{-}2)$$

Using (15-1) and (16-2), we have that

$$(NE\Delta T_A^{New})_{L,\ Scenario\ 3} < NE\Delta T_{C_W}^{ICVS}. \quad (17)$$

(17) means that for a post-launch instrument, the magnitude of the instrument noise calculated using the ICVS method is higher than that using the new method.

Based the above analysis, we can easily reveal the similar conclusions for the Hans method. The Hans method in (3) computes the noise based on a linear interpolation of cold and warm count noise components, $NE\Delta T_{C_W}^{ICVS}$ and $NE\Delta T_{C_C}^{ICVS}$, where each of them is computed using a scheme similar to the ICVS method. For the first two scenarios, i.e., a noise-free instrument or a pre-launch instrument, the noise contribution from the cold count and the warm count is either zero or the same. The Hans method is exchangeable with the ICVS method and the new method. For Scenario 3, we can approve that $NE\Delta T_{C_C}^{ICVS} > (NE\Delta T_A^{New})_{L,\ Scenario\ 3}$. In combination with (17), we have

$$NE\Delta T_{C_W}^{ICVS} > (NE\Delta T_A^{New})_{L,\ Scenario\ 3} > NE\Delta T_{C_C}^{ICVS}. \quad (18)$$

However, as given in (3) above, $NE\Delta T_A^{Hans}$ is a linear interpolation between $NE\Delta T_{C_C}^{ICVS}$ and $NE\Delta T_{C_W}^{ICVS}$ based on the relative distance of earth scene temperature T_A to two calibration temperatures T_W and T_C. Because T_A is very close to T_W, the magnitude of $NE\Delta T_A^{Hans}$ is actually closer to $NE\Delta T_{C_W}^{ICVS}$. The analysis in Section V will reveal that $NE\Delta T_A^{Hans}$ is still larger than that using the new method.

Briefly, the new formula has demonstrated improvements over the existing ICVS and Hans methods. It is capable for quantifying the temperature dependency of the instrument noise performance. More importantly, it takes into account all major noise components occurred in calibration parameters for an on-orbit AMSU-A instrument, each of which is computed using the accurate sensitivity. In the following section, the noise errors for onboard AMSU-A instruments by using the ICVS and Hans methods are further quantified in comparison with the new method.

V. On-Orbit Noise Performance Assessment Using Three Noise Methods

The deficiency in the existing gain-based methods such as the ICVS method [11] and the Hans method [14] is theoretically addressed above. Below, we apply the ICVS, Hans and new methods to AMSU-A instruments onboard NOAA-18 to -19 and Metop-A to –C to quantify the differences of the orbital averaging noises between the existing and new methods for AMSU-A instruments.

A. Application to Four Legacy AMSU-A Instruments

For the four legacy instruments, we select the same data sets as those using in Section III-B above. Figs. 5 through 8 display the time series of $(NE\Delta T_A^{New})_L$, $(NE\Delta T_{C_W}^{New})_L$, $NEDT_{C_W}^{ICVS}$ and $NE\Delta T_A^{Hans}$ for channel 2 (AMSU-A2); channel 5 or 8 (AMSU-A1-2); and channel 9 (AMSU-A1-1) onboard NOAA-18, NOAA-19, Metop-A, and Metop-B. Here, $(NE\Delta T_{C_W}^{New})_L$ represents the warm noise component in the new method and the superscript 'New' is added to distinguish it from $NE\Delta T_{C_W}^{ICVS}$. The channels in the figure are chosen to include at least one channel associated with each antenna sub-unit system since anomalies of calibration parameters are naturally associated with each specific antenna system.

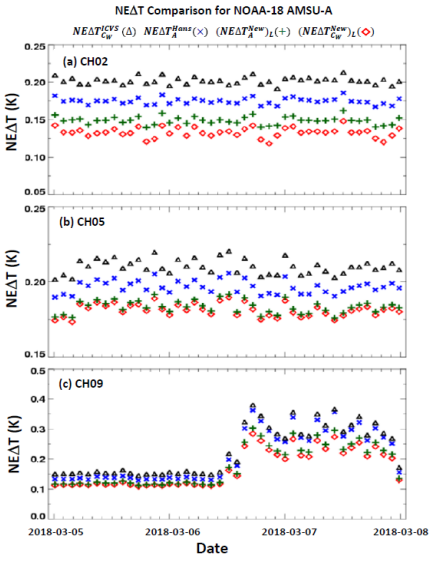

Fig. 5. Time series of orbital $(NE\Delta T_A^{New})_L$ (green plus), $(NE\Delta T_{C_W}^{New})_L$ (red diamond), $NEDT_{C_W}^{ICVS}$ (black triangle), and $NEDT_{C_W}^{Hans}$ (blue crosshair) for three NOAA-18 AMSU-A channels during three days of the data sets. The symbols in the figure are applicable for Figs. 6 through 8 and 'date' in the X-axis is given in the format of year-month-day. (a) Channel 2. (b) Channel 5. (c) Channel 9.

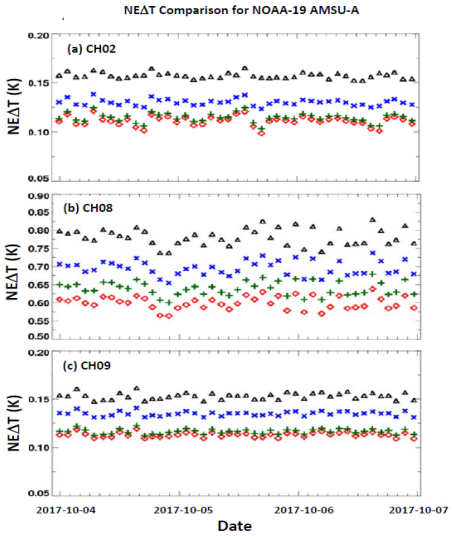

Fig. 6. Same as Fig. 5 except for NOAA-19 with slightly different channels. (a) Channel 2. (b) Channel 8. (c) Channel 9.

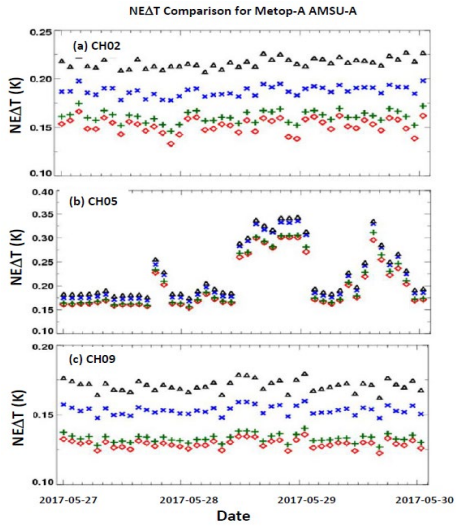

Fig. 7. Same as Fig. 5 except for Metop-A.

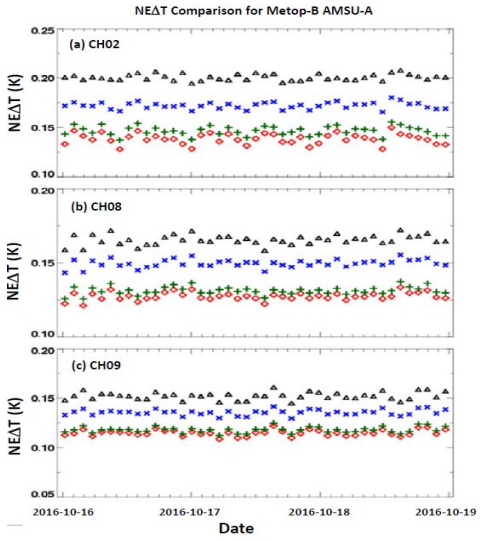

Fig. 8. Same as Fig. 5 except for Metop-B with slightly different channels. (a) Channel 2. (b) Channel 8. (c) Channel 9.

For all displayed channels and satellite instruments, the orbital averages of $NEDT_{C_W}^{ICVS}$ and $NE\Delta T_A^{Hans}$ are consistently higher than those of $(NE\Delta T_A^{New})_L$. This conclusion is qualitatively consistent with the analysis in Section IV, but the discrepancy amount varies with channel and satellite instrument. For the NOAA-18 AMSU-A, $NEDT_{C_W}^{ICVS}$ at channels 2, 5, and 9 can be larger than the $(NE\Delta T_A^{New})_L$ by approximately 35%, 13% and 26% correspondingly; for NOAA-19 AMSU-A, the $NEDT_{C_W}^{ICVS}$ at channels 2, 8, and 9 by approximately 37%, 22% and 31% correspondingly; for Metop-A AMSU-A, the $NEDT_{C_W}^{ICVS}$ at channels 2, 5, and 9 by approximately 35%, 11% and 28% correspondingly; for Metop-B AMSU-A, the $NEDT_{C_W}^{ICVS}$ at channels 2, 8, and 9 by approximately 37%, 26% and 29% correspondingly. Similar errors exist for $NE\Delta T_A^{Hans}$ against the new method but with decreased magnitude. The Hans method overestimates the amount of the instrument noise against the new method by approximately 5% to 17%. This is understandable because $NE\Delta T_A^{Hans}$ is evaluated based on a linear interpolation from $NE\Delta T_{C_C}^{ICVS}$ and $NE\Delta T_{C_W}^{ICVS}$.

Additionally, it is interesting to compare $NEDT_{C_W}^{ICVS}$ against $(NE\Delta T_{C_W}^{New})_L$ because both of them use the Allan deviation of warm counts. Compared with instrument noise (i.e., $(NE\Delta T_A^{New})_L$), $NEDT_{C_W}^{ICVS}$ differs more from the warm noise component. For example, instrument noise from the ICVS method is greater than that found from the new method (i.e., $(NE\Delta T_{C_W}^{New})_L$) by approximately 53%, 41%, 43% and 45% at channel 2 for AMSU-A instruments onboard NOAA-18, NOAA-19, Metop-A and Metop-B correspondingly. This dissimilarity is due to the use of a different sensitivity for the transformation of the warm count Allan deviation into NEΔT:

$$(NE\Delta T_{C_W}^{New})_L = \frac{\left(\sigma_{C_W}^{A}\right)_L}{\left|\left(\frac{\partial T_A}{\partial C_W}\right)_L\right|^{-1}} < NE\Delta T_{C_W}^{ICVS} \quad \text{because} \quad G_0 < \left|\left(\frac{\partial T_A}{\partial C_W}\right)_L\right|^{-1}.$$

Table III Three day-means and/or percentages of $(NE\Delta T_A^{New})_L$, $(NE\Delta T_{C_W}^{New})_L$, $NEDT_{C_W}^{ICVS}$ and $NE\Delta T_A^{Hans}$ at 15 channels for Metop-B AMSU-A. The percentage of each noise component is defined as $\frac{NE\Delta T_X}{(NE\Delta T_A^{New})_L} \times 100\%$, where $(NE\Delta T_A^{New})_L$ is calculated using (8) and $NE\Delta T_X$ denotes one of $(NE\Delta T_{C_W}^{New})_L$, $NEDT_{C_W}^{ICVS}$, and $NE\Delta T_A^{Hans}$.

Ch.#	$(NE\Delta T_A^{New})_L$	$(NE\Delta T_{C_W}^{New})_L$		$NEDT_{C_W}^{ICVS}$		$NE\Delta T_A^{Hans}$	
	(K)	(K)	(%)	(K)	(%)	(K)	(%)
1	0.136	0.129	94.9	0.183	134.6	0.159	116.9
2	0.147	0.139	94.6	0.201	136.8	0.172	117.0
3	0.222	0.219	98.6	0.255	114.9	0.238	107.2
4	0.140	0.138	98.6	0.153	109.3	0.147	105.0
5	0.127	0.126	99.2	0.143	112.6	0.135	106.3
6	0.110	0.108	98.2	0.132	120.0	0.120	109.1
7	0.110	0.108	98.2	0.137	124.5	0.124	112.7
8	0.131	0.128	97.7	0.166	126.7	0.150	114.5
9	0.118	0.115	97.5	0.153	129.7	0.136	115.3
10	0.156	0.153	98.1	0.200	128.2	0.178	114.1
11	0.177	0.175	98.9	0.221	124.9	0.198	111.9
12	0.264	0.261	98.9	0.319	120.8	0.291	110.2
13	0.377	0.375	99.5	0.438	116.2	0.407	108.0
14	0.639	0.637	99.7	0.716	112.1	0.677	105.9
15	0.119	0.116	97.5	0.136	114.3	0.130	109.2

Other channels also show similar features to these at the abovementioned channels. For instance, Tables III displays the three-day mean of $(NE\Delta T_A^{New})_L$, $(NE\Delta T_{C_W}^{New})_L$, $NE\Delta T_{C_W}^{ICVS}$ and $NE\Delta T_A^{Hans}$ at all available channels for AMSU-A aboard Metop-B. For all channels, the instrument noise calculated using the ICVS method is larger than that using the new method by approximately from 8% to 37%. The instrument noise found by using the Hans method is larger than that found by using the new method by approximately 5% to 18%. In

particular, the two window channels from 1 to 2 exhibit the biggest difference because they observe large differences between the Earth-scene and warm load temperatures over oceans. Similar conclusion is observed at the other three legacy AMSU-A instruments (the tables are omitted).

Therefore, in comparison with the new method, the existing ICVS and Hans methods persistently overrate the noise of AMSU-A instruments onboard the legacy NOAA-18 to NOAA-19 and Metop-A to Metop–B. The two window channels, 1 and 2, exhibit the largest errors that are about 0.05K for the ICVS or 0.25K for the Hans method. The relative errors are more than 30% for the ICVS method or more than 15% for the Hans method. The errors are also notable for temperature sounding channels.

B. Application to Metop-C AMSU-A Instrument

The (Metop-C) satellite, which was launched into low Earth orbit on November 6, 2018, carries the last NOAA AMSU-A. On November 15, 2018, nine days after launch of the Metop-C satellite, the first day AMSU-A science data was received. In this study, we analyze the lifetime noise performance since November 15, 2018 by using the ICVS and new methods respectively. The Hans method is similar to the ICVS method, so it is not included here.

According to our computations, the Metop-C AMSU-A demonstrates a relatively stable noise performance since the activation of the instrument for all channels except for the channel 3. Figs. 9(a) to 9(f) display the time series of on-orbit $NE\Delta T$ at six AMSU-A channels since November 15, 2018 through June 20, 2020, by using the two methods. The AMSU-A noises at the majority of the channels are continuously within the specification, where the specifications are referred to [1]. The channel 3 noise is unstable with time: it was mostly within the specification (0.4K) prior to April 7 2019, but it gradually rises to the order of 1 K significantly exceeding the specification since then. The channel 7 also exhibited a big jump exceeding the specification of 0.25K on May 12 and 25, 2019 respectively. A few anomalous noise events occurred at other channels during the monitored period, but resultant noise magnitudes are constantly within the specification. Those features are well caught by the two methods.

On the other hand, our results show that for Metop-C AMSU-A, the ICVS method persistently overestimates the on-orbit noise against the new method by approximately 11% to 38% depending on channel during the monitored period, as shown in Figs. 9(a) to 9(f), which are similar to what we observed for other legacy AMSU-A instruments above. Fig. 9(g) presents the averaged noise magnitude over the monitored period at the 15 channels using the two methods. Among all channels, the ICVS method produces large positive noise estimation errors in the first three channels compared with the new method. For example, the ICVS method causes an absolute error of 0.07K in channel 3. The upper temperature sounding channels 10 – 14 are important for applications especially in numerical weather prediction (NWP), where an error of around 0.05K occurs. Those errors indicate the improvement of noise estimate accuracy using the new method.

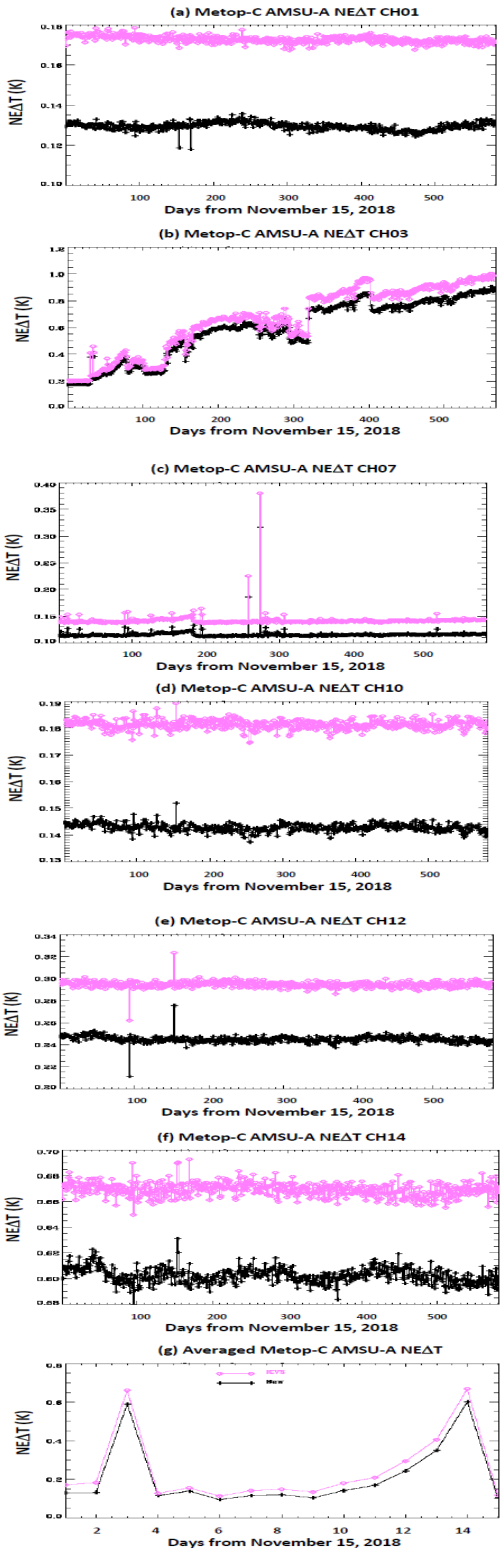

Fig. 9 Time series of on-orbit $NE\Delta T$ at several channels for Metop-C AMSU-A since 15 Nov. 2018 through 20 June 2020 from (a) to (f) and the averaged $NE\Delta T$ vs. channel for (g), using the ICVS (pink or line crossed with 'diamond') and new methods (black or line crossed with '+'). The different dynamic range in y-axis is used to highlight

the variation of noise; the x-axis is the number of days since November 15, 2018. (a) Ch. 1. (b) Ch. 3. (c) Ch. 7. (d) Ch. 10. (e) Ch. 12. (f) Ch. 14. (g) Averaged $NE\Delta T$ vs. channel.

In summary, the new method improves the accuracy of noise calculations at 15 channels for Metop-C AMSU-A instrument. Relatively large improvement occurs at the channels from 1 to 3 and the upper temperature sounding channels from 10 to 14 that are critical in NWP models. Therefore, along with the analysis for legacy AMSU-A instruments, the results highlight the significance of the noise computations using the newly derived method for all AMSU-A instruments.

VI. Summary and Conclusions

This study establishes a new methodology for on-orbit AMSU-A instrument noise calculation by taking into account the major noise components resulting from calibration parameters, e.g., the warm radiometric count noise component, the warm target temperature noise component, the cold radiometric count noise component, and their covariance. It is capable for evaluating the temperature dependency of a post-launch instrument noise performance, which is difficult if not impossible using the existing methods. In addition, each noise component in the new method is accurately computed using the sensitivity of each calibration parameter to temperature instead of the gain that is used in the existing methods.

Moreover, the new formula quantifies the error in the ICVS and Hans methods in estimating instrument noise for AMSU-A instruments onboard NOAA-18, NOAA-19 and Metop-A to Metop-C. Specifically, the lifetime noise performance of Metop-C AMSU-A instrument is analyzed. According to our results, for the five legacy AMSU-A instruments, the ICVS method consistently overestimates AMSU-A instrument noise in comparison with the new method by approximately 8% to 37% depending upon channel and satellite, which are error of approximately 0.02 to 0.07 K. Similarly, the Hans method overrates the instrument noise by approximately 5% to 18%. In addition, the Metop-C AMSU-A instrument demonstrates a relatively stable noise performance since the launch for all channels except for the channel 3, which are confirmed by either the new or ICVS method.

The new method has demonstrated persistent improvements in estimating AMSU-A instruments onboard the five satellites from NOAA-18 to NOAA-19, Metop-A to Metop–C. In fact, the formula is also applicable to other satellite instruments for which calibration is based on warm and cold targets such as ATMS and MHS. The new noise formula is given in a domain of temperature instead of the domain of radiance. The resultant noise errors in the temperature domain instead of the radiance domain are approximately 0.1% to 0.5% at AMSU-A frequencies. However, the errors can be increased to approximately 0.8% for 157GHz, 0.8% for 183GHz, 0.96% for 300GH, given that $T_W = 280K, T_C = 2.73K$. Although the absolute noise errors are still trivial at a very high frequency, it is recommended that the computation of the noise is made at the radiance domain for a microwave instrument with very high frequencies. This also can comply with a calibration equation in the domain of radiance, which is especially important for a microwave instrument with high frequencies [23]. In spite of those advantages, the new method does not consider the contribution of the noise in earth scene counts (C_S) because of the challenge to distinguish the noise portion from the signal portion relevant to atmospheric and/or surface features in C_S. Certain errors could be contributed to the on-orbit instrument noise computation. A separate study would be conducted by using a principle component method to further improve the accuracy of on-orbit instrument noise computation.

Appendix A Derivation of New Noise Computation Formula

In AMSU-A SDR data file, the radiometer output, the antenna temperature of an Earth-scene, T_A, is determined using a nonlinear calibration equation, i.e., [15]-[17]

$$T_A = T_W + (T_W - T_C)\frac{(C_S - C_W)}{(C_W - C_C)} + \mu(T_W - T_C)^2\frac{(C_S - C_W)(C_S - C_C)}{(C_W - C_C)^2}, \quad \text{(A1)}$$

where $C_C, C_W\ and\ C_s$ denote the cold space, warm target and Earth-scene radiometric counts respectively; T_C and T_W denote the cold space and warm target PRT temperatures respectively; and μ denotes the nonlinear coefficients. The indices of channel and scan line are regularly omitted in (1) and subsequent equations throughout the manuscript for clarity.

According to the propagation of error formulas [19], for a function with multiple variables (e.g., $F(x, y, z)$), with higher order terms neglected, the variance of $F(x, y, z)$ can be expressed by the following equation.

$$\sigma_F^2 = \left[\frac{\partial F}{\partial x}\right]^2\sigma_x^2 + \left[\frac{\partial F}{\partial y}\right]^2\sigma_y^2 + \left[\frac{\partial F}{\partial z}\right]^2\sigma_z^2 + 2\frac{\partial F}{\partial x}\cdot\frac{\partial F}{\partial y}\cdot cov(x,y) + 2\frac{\partial F}{\partial x}\cdot\frac{\partial F}{\partial z}\cdot cov(x,z) + 2\frac{\partial F}{\partial y}\cdot\frac{\partial F}{\partial z}\cdot cov(y,z), \quad \text{(A2)}$$

where σ_x^2, σ_y^2 and σ_z^2 are the variances of *x, y,* and *z* respectively; $cov(x,y)$, $cov(x,z)$, and $cov(y,z)$ are the covariance of *x* and *y, x* and *z,* and *y* and *z* respectively; $\frac{\partial F}{\partial x}, \frac{\partial F}{\partial y}$, and $\frac{\partial F}{\partial z}$ are the partial derivatives of F with respect to *x, y,* and *z* respectively.

In light of (A1), T_A is the function of three calibration parameters, i.e., $F(x, y, z) = T_A(C_W, C_C, T_W)$. With Eqs. (A1) and (A2), we have the following equation

$$NE\Delta T_A^{New} = \sigma_{T_A}^A = \sqrt{(NE\Delta T_{C_W})^2 + (NE\Delta T_{C_C})^2 + (NE\Delta T_{T_W})^2 + \delta_{Cov(C_W,C_C)} + \delta_{Cov(C_W,T_W)} + \delta_{Cov(C_C,T_W)}}. \quad \text{(A3)}$$

with

$$NE\Delta T_{C_W} = \left|\frac{\partial T_A}{\partial C_W}\sigma_{C_W}^A\right|, \quad \text{(A4-1)}$$

$$NE\Delta T_{C_C} = |\frac{\partial T_A}{\partial C_C}\sigma_{C_C}^A|, \quad \text{(A4-2)}$$

$$NE\Delta T_{T_W} = \left|\frac{\partial T_A}{\partial T_W}\sigma_{T_W}^A\right|, \quad \text{(A4-3)}$$

$$\delta_{Cov(C_W,C_C)} = 2\frac{\partial T_A}{\partial C_W}\frac{\partial T_A}{\partial C_C}cov(C_W,C_C), \quad \text{(A4-4)}$$

$$\delta_{Cov(C_W,T_W)} = 2\frac{\partial T_A}{\partial C_W}\frac{\partial T_A}{\partial T_w}cov(C_W,T_W), \quad \text{(A4-5)}$$

$$\delta_{Cov(C_C,T_W)} = 2\frac{\partial T_A}{\partial C_c}\frac{\partial T_A}{\partial T_W}cov(C_C,T_W), \quad \text{(A4-6)}$$

$$\frac{\partial T_A}{\partial T_W} = 1 + \frac{(C_S-C_W)}{(C_W-C_C)} + 2\mu(T_W-T_C)\frac{(C_S-C_W)(C_S-C_C)}{(C_W-C_C)^2}, \quad \text{(A4-7)}$$

$$\frac{\partial T_A}{\partial C_W} = \frac{(T_W-T_C)(C_C-C_S)}{(C_W-C_C)^2} + \mu(T_W-T_C)^2(C_S-C_C)\frac{(C_C-2C_S+C_W)}{(C_W-C_C)^3}, \quad \text{(A4-8)}$$

$$\frac{\partial T_A}{\partial C_C} = \frac{(T_W-T_C)(C_S-C_W)}{(C_W-C_C)^2} - \mu(T_W-T_C)^2(C_S-C_W)\frac{(C_C-2C_S+C_W)}{(C_W-C_C)^3}, \quad \text{(A4-9)}$$

where all of three derivatives are a function of scene count (C_S) or scene temperature (T_A) via (A1) thus resulting in the dependency of instrument noise on temperature. In particular, $(NE\Delta T_A)_{NL}$ represents the composite contribution of all noise components to $NE\Delta T_A^{New}$ as the three derivatives in (A4-7) through (A4-9) only contain the nonlinear part with nonlinear coefficient μ.

The "variance" of each variable in (A2) are replaced by its corresponding overlapping Allan deviation, e.g., $\sigma_{C_W}^A, \sigma_{C_C}^A, \sigma_{T_W}^A$. The overlapping Allan deviation for each of the calibration parameters is expressed as

$$\sigma_{\mathrm{y}}^A = \sqrt{\frac{1}{2(N-2)}\sum_{i=1}^{N-1}(y_{i+1}-y_i)^2}, \quad \text{(A5)}$$

where the parameter 'y' denotes one of C_C, C_W and T_W; the superscript 'A' the Allan deviation ('overlapping' is hereinafter omitted for simplification); 'i' the index of scan; 'N' the total number of scans per orbit. In other words, each statistical parameter is calculated based on an average of observations per orbit by following the current ICVS method [11]. Three covariance parameters, i.e., $cov(T_W,C_W), cov(C_W,C_C), cov(C_C,C_W)$, represent the covariances between two of the following: cold count, warm count, and warm blackbody temperature instabilities.

In summary, the instrument noise in (A3) consists of six noise components. The three independent components, $NE\Delta T_{C_W}$, $NE\Delta T_{C_C}$, and $NE\Delta T_{T_W}$, are hereinafter termed the warm count noise, cold count noise, and warm PRT temperature noise for clarity unless otherwise mentioned. The other three noise components consist of covariance items (i.e., $\delta_{Cov(C_W,C_C)}$, $\delta_{Cov(C_W,T_W)}$, and $\delta_{Cov(C_C,T_W),}$) which can be positive or negative depending on proportional or inverse relationships among the relevant parameters. Each noise component involves computation of nonlinear items via derivatives as shown in (A4-7) through (A4-9).

APPENDIX B. COMPUTATION EXPRESSIONS OF ORBITAL AVERAGED $NE\Delta T_A^{New}$ IN (6) FOR AMSU-A OBSERVATIONS

The $NE\Delta T_A^{New}$ defined in (6) is rewritten here.

$$NE\Delta T_A^{New} = \sqrt{\left(NE\Delta T_{C_W}\right)^2 + \left(NE\Delta T_{C_C}\right)^2 + \left(NE\Delta T_{T_W}\right)^2 + \delta_{Cov(C_W,C_C)} + \delta_{Cov(C_W,T_W)} + \delta_{Cov(C_C,T_W)}}. \quad \text{(B1)}$$

We calculated each $NE\Delta T$-component by averaging over N scans in one orbit by using each sample-based Allan deviation, which is consistent with the ICVS AMSU-A operational noise calculation procedure. Among AMSU-A observations, there are 2 samples of cold and warm count measurements per scan for AMSU-A1 and -A2. For AMSU-A1, which includes channels 3-15, there are 5 measurement samples of warm load PRT temperatures per scan. For AMSU-A2, which includes channels 1 and 2, there are 7 samples of warm load PRT temperatures per scan [21]. Therefore, the three independent noise components in the $NE\Delta T_A^{New}$ can be computed as follows.

$$\left(NE\Delta T_{T_W}\right)^2 = \frac{1}{2K(N-2)}\sum_{i=1}^{N-1}\overline{\left(\frac{\partial T_A(i)}{\partial T_W(i)}\right)}^2\sum_{k=1}^{K}\left(T_{W_k}(\mathrm{i}+1) - T_{W_k}(\mathrm{i})\right)^2, \quad \text{(B2)}$$

$$\left(NE\Delta T_{C_W}\right)^2 = \frac{1}{4(N-2)}\sum_{i=1}^{N-1}\overline{\left(\frac{\partial T_A(i)}{\partial C_W(i)}\right)}^2\left[\left(C_{W_1}(\mathrm{i}+1) - C_{W_1}(\mathrm{i})\right)^2 + \left(C_{W_2}(\mathrm{i}+1) - C_{W_2}(\mathrm{i})\right)^2\right], \quad \text{(B3)}$$

$$\left(NE\Delta T_{C_C}\right)^2 = \frac{1}{4(N-2)}\sum_{i=1}^{N-1}\overline{\left(\frac{\partial T_A(i)}{\partial C_C(i)}\right)}^2\left[\left(C_{C_1}(\mathrm{i}+1) - C_{C_1}(\mathrm{i})\right)^2 + \left(C_{C_2}(\mathrm{i}+1) - C_{C_2}(\mathrm{i})\right)^2\right], \quad \text{(B4)}$$

where K is a number of PRT temperatures depending on channel and K= 5 for AMSU-A1 or K = 7 for AMSU-A2. The $\overline{\frac{\partial T_A}{\partial T_W(i)}}, \overline{\frac{\partial T_A}{\partial C_W(i)}}, and\ \overline{\frac{\partial T_A}{\partial C_C(i)}}$ denote the scan-averaged derivatives. In particular, as the non-linear items can be neglected, those derivatives are calculated the following equations.

$$\frac{\partial T_A(i)}{\partial T_W(i)} \approx \left(\overline{\frac{\partial T_A(i)}{\partial T_W(i)}}\right)_L = 1.0 + \frac{\overline{(C_S(i)-C_W(i))}}{\overline{(C_W(i)-C_C(i))}}, \quad \text{(B5)}$$

$$\frac{\partial T_A(i)}{\partial C_W(i)} \approx \left(\overline{\frac{\partial T_A(i)}{\partial C_W(i)}}\right)_L = \frac{\overline{(T_W(i)-T_C(i))(C_C(i)-C_S(i))}}{\overline{(C_W(i)-C_C(i))^2}}, \quad \text{(B6)}$$

$$\frac{\partial T_A(i)}{\partial C_C(i)} \approx \left(\overline{\frac{\partial T_A(i)}{\partial C_C(i)}}\right)_L = \frac{\overline{(T_W(i)-T_C(i))(C_S(i)-C_W(i))}}{\overline{(C_W(i)-C_C(i))^2}}. \quad \text{(B7)}$$

Similarly, we obtained the formula about covariance terms as described as follows.

$$\delta_{Cov(C_W,T_W)} = \frac{1}{4(N-2)}\sum_{i=1}^{N-1}\overline{\frac{\partial T_A(i)}{\partial C_W(i)}}\cdot\overline{\frac{\partial T_A(i)}{\partial T_W(i)}} \cdot\left(\overline{T_W}(i+1) - \overline{T_W}(i)\right)\times \times\left\{\sum_{i=1}^{2}\left(C_{W_k}(i+1) - C_{W_k}(i)\right)\right\} \quad \text{(B8)}$$

$$\delta_{Cov(C_C,T_W)} = \frac{1}{4(N-2)}\sum_{i=1}^{N-1}\overline{\frac{\partial T_A(i)}{\partial C_C(i)}}\cdot\overline{\frac{\partial T_A(i)}{\partial T_W(i)}} \cdot\left(\overline{T_W}(i+1) - \overline{T_W}(i)\right)\times\times\left\{\sum_{k=1}^{2}\left(C_{C_k}(i+1) - C_{C_k}(i)\right)\right\} \quad \text{(B9)}$$

$$\delta_{Cov(C_W,C_C)} = \frac{1}{4(N-2)}\sum_{i=1}^{N-1}\overline{\frac{\partial T_A(i)}{\partial C_W(i)}}\cdot\overline{\frac{\partial T_A(i)}{\partial C_C(i)}}\times \times\left\{\sum_{k=1}^{2}\left(C_{W_k}(i+1)-C_{W_k}(i)\right)\left(C_{C_k}(i+1)-C_{C_k}(i)\right)\right\} \quad \text{(B10)}$$

$$\overline{T_W}(i) = \frac{1}{K}\sum_{k=1}^{K} T_{W_k}(i). \quad \text{(B11)}$$

Additionally, as only the nonlinear items are considered, (B1) is rewritten to be

$$(NE\Delta T_A)_{NL} = \sqrt{\left(NE\Delta T_{T_W}\right)_{NL}^2 + \left(NE\Delta T_{C_W}\right)_{NL}^2 + \left(NE\Delta T_{C_C}\right)_{NL}^2 + (\delta_{COV})_{NL}} \quad \text{(B12)}$$

where the computation of each item is similar to corresponding one in (B1) except for removing the items without the nonlinear parameter μ in the computations of $\frac{\partial T_A}{\partial T_W}$, $\frac{\partial T_A}{\partial C_W}$ and $\frac{\partial T_A}{\partial C_C}$ [see $(A4-7)\sim(A4-9)$].

ACKNOWLEDGMENT

The authors would like to thank the NOAA Center for Satellite Applications and Research (STAR) for supporting NOAA legacy Advanced Microwave Sounding Unit –A (AMSU-A) instrument calibration/validation and the NOAA Office of Projects, Planning, and Analysis (OPPA) for supporting Metop-C AMSU-A calibration/validation. The authors would also like to thank Dr. Ninghai Sun for writing the code used to read AMSU-A SDR data. Thanks go to Drs. Changyong Cao and Cheng-Zhi Zou for their very useful scientific comments. Thanks go to Dr. Haifeng Qian for his providing useful discussion about prelaunch noise computation. Thanks further go to Mr. Warren Porter and Dr. Ryan Stanfield for their proofreading the manuscript for grammar and spelling. The last but not least, thank go to two anonymous reviewers for providing excellent comments.

REFERENCES

[1] Northrop Grumman Electronic Systems (NGES) technique report NAS 5-32314 CDRL 307 (2010), AMSU-A System Operation and Maintenance Manual for FOR METSAT/METOP, S/N 105 through 109

[2] J. C. Derber, Wu, W. S., "The use of TOVS cloud-cleared radiances in the NCEP SSI analysis system. Mon. Weather Rev.," 126, 2287 – 2299, 1998.

[3] G. Kelly, and Thépaut, J.-N., "Evaluation of the impact of the space component of the Global Observation System through observing system experiments," ECMWF Newsletter, No. 113, ECMWF, Reading, United Kingdom, 16–28, http://www.ecmwf.int/publications/newsletters/pdf/113.pdf, 2017.

[4] B. Yan and F. Weng, "Effects of Microwave Desert Surface Emissivity on AMSU-A Data Assimilation, IEEE Transactions on Geoscience and Remote Sensing," 49, 1263 - 1276, 10.1109/TGRS.2010.2091508, 2011.

[5] X. L. Zou, "Climate trend detection and its sensitivity to measurement precision," Adv. Meteorol. Sci. Technol., 2, 41–43, 2012.

[6] X. L. Zou, Qin Z. and Weng F., "Impacts from assimilation of one data stream of AMSU-A and MHS radiances on quantitative precipitation forecasts," Q. J. R. Meteorol. Soc. 143, 731–743, B DOI:10.1002/qj.2960, 2017.

[7] S. A. Boukabara, Garrett, K., Chen, W. C., Iturbide-Sanchez, F., Grassotti, C., Kongoli, C., Chen, R. Y., Liu, Q. H., Yan, B. H.,Weng, F. Z., Ferraro, R., Kleespies, T. J., and H. Meng, " MiRS: An All-Weather 1DVAR Satellite Data Assimilation and Retrieval System," IEEE Transactions on Geoscience and Remote Sensing, 49, 3249-3272, 10.1109/tgrs.2011.2158438, 2011.

[8] C. Z. Zou and Wang W., "Intersatellite calibration of AMSU-A observations for weather and climate applications," J. G. R., 116, D23113, 2011.

[9] G. Ohring, Wielicki B., Spencer R., Emery B., and Datla R., "Satellite instrument calibration for measuring global climate change: Report of a workshop," Bull. Amer. Meteorol. Soc., 86, 1303–1313, 2005.

[10] B. Wielicki, D. F. Young, and M. G. Mlynczak, "Achieving climate change absolute accuracy in orbit," Bull. Amer, Meteorol. Soc., 94, 1519–1539, 2013.

[11] M. Tian, Zou, X., and Weng, F., "Use of Allan Deviation for Characterizing Satellite Microwave Sounder Noise Equivalent Differential Temperature (NEDT)," 12, 2477–2480, https://doi.org/10.1109/LGRS.2015.2485945, 2015.

[12] D. W. Allan: Statistics of atomic frequency standards, Proceedings of the IEEE, 54, 221–230, 1966.

[13] D. W. Allan, "Should classical variance be used as a basic measure in standards metrology?" IEEE Trans. Instrum. Meas., 36, 646–654, 1987.

[14] I. Hans, M. Burgdorf1, V. O. John, J. Mittaz, and S. A. Buehler, "Noise performance of microwave humidity sounders over their life Time," Atmos. Meas. Tech., 10, 4927–4945, https://doi.org/10.5194/amt-10-4927-2017, 2017.

[15] T. Mo, "AMSU-A Antenna Pattern Corrections," IEEE Trans. Geoscience and Remote Sen., 37, 1999.

[16] T. Mo, "Prelaunch calibration of the advanced microwave sounding Unit-A for NOAA-K," IEEE Trans. Microwave Theory Tech., 44, 1460–1469, doi:10.1109/22.536029, 1996.

[17] NOAA Technical Report NESDIS 121, "Calibration of the Advanced Microwave Sounding Unit-A Radiometer for METOP-A," Washington, D.C, August 2006

[18] F. Weng, Zou X., Sun N., Yang H., Tian M., Blackwell, W. J., Wang X., Lin L., and Anderson K., "Calibration of Suomi National Polar-orbiting Partnership Advanced Technology Microwave Sounder," J. Geophys. Res.: Atmospheres, 118, 11 187–11 200, 2013.

[19] H. Ku, "Notes on the Use of Propagation of Error Formulas," J. Research of National Bureau of Standards-C Engineering and Instrumentation, 70C, 263-273, 1966.

[20] F. T., Ulaby, Long, D. G., W. Blackwell, C. Elachi, A. Fung, C. Ruf, K. Sarabandi, H. Zebker, and J. Zy, "Microwave Radar and Radiometric Remote Sensing," University of Michigan Press, 1st University of Michigan Press, ISBN: 978-0-472-11935-6, 263-279, January 2014.

[21] Northrop Grumman Electronic Systems (NGES) technique report NAS 5-32314, "Integrated Advanced Microwave

Sounding Unit-A (AMSU-A) Calibration Log Book," S/N 105, August 2010.
[22] B. Yan, J. Chen, C. Zou, and co-authors, "Calibration and Validation of Metop-C Advanced Microwave Sounding Unit-A (AMSU-A) Antenna and Brightness Temperatures", submitted to Remote Sensing, 2020.
[23] F. Weng and X. Zou, "Errors from Rayleigh–Jeans approximation in satellite microwave radiometer calibration systems," Applied Optics, 52, 505-508, 2013.

Banghua Yan received the Ph.D. degree in atmospheric physics from the Institute of Atmospheric Physics, Chinese Academy of Sciences, Beijing, China, in 1997 and the Ph.D. degree in atmospheric radiation from the University of Alaska, Fairbanks, in 2001. She is currently a physical scientist with the Satellite Calibration and Data Assimilation Branch in the NOAA Center for Satellite Applications and Research (STAR). From November 1999 to July 2010, she worked for the STAR through companies or NOAA Joint Center for Satellite Data Assimilation (JCSDA) or the Earth System Science Interdisciplinary Center in University of Maryland. During this period, she significantly contributed to the developments of microwave land, snow, and sea ice emissivity models, and microwave satellite instrument data assimilation studies. Those work have significantly improved the use of satellite sounding data in numerical weather prediction (NWP) models. The land, snow, and sea ice microwave emissivity models have been implemented into the NOAA NCEP NWP model and the JCSDA community radiative transfer model that has been successfully used in several operational data assimilation systems in the U.S. From August 2010 to August 2018, she was an Oceanographer with the NOAA Office of Satellite Data Processing and Distribution, Camp Springs, MD, to lead the NOAA operational ocean color production system. She has published approximately 30 papers in international peer-reviewed journals as the first or co-author. Currently, she leads calibrations/validations of Metop-C AMSU-A and Joint Polar Satellite System Ozone Mapping and Profiler Suite (OMPS), and the STAR Integrated Calibration/Validation System (ICVS) Long-term Monitoring. She also coordinated the JPSS/STAR (JSTAR) mission program for more than half years.

Stanislav V. Kireev received M.S. degree in physics from the Moscow State University, Russia, in 1986 and the Ph.D. degree in atmospheric science from the Institute of Atmospheric Physics, Moscow, Russian Academy of Sciences, in 1997. From 2002 to 2014, he was a Research Assistant Professor with the Center for Atmospheric Sciences, Hampton University, VA. Since 2016, he is a scientist with Global Science and Technology, Inc. for NOAA/STAR. His research interests include the remote sensing of the atmosphere, development of forward models and retrieval algorithms, satellite instrument calibration and validation. He is the author and co-author of more than 50 articles and presentations in the field.